

Original Article

3D-QSAR, DOCKING STUDY, PHARMACOPHORE MODELING AND ADMET PREDICTION OF 2-AMINO-PYRAZOLOPYRIDINE DERIVATIVES AS POLO-LIKE KINASE 1 INHIBITORS

JAIPRAKASH N. SANGSHETTI^{1*}, FIROZ A. KALAM KHAN¹, YASAR Q. QAZI¹, MANOJ G. DAMALE², ZAHID ZAHEER¹

¹Rafiq Zakaria Campus, Y.B. Chavan College of Pharmacy, Aurangabad 431001 (MS) India, ²MGM's Institute of Biosciences and Technology, Aurangabad 431003 (MS) India.
Email: jnsangshetti@rediffmail.com

Received: 30 Jun 2014 Revised and Accepted: 04 Aug 2014

ABSTRACT

Objective: The polo-like kinase 1 (plk1) plays important roles in the regulation of mitotic progression, including mitotic entry, spindle formation, chromosome segregation and cytokinesis. Thus, plk1 is considered as a good target for chemotherapeutic intervention. The main objectives of this research were to *in silico* screen the 2-amino-pyrazolopyridine derivatives as plk1 inhibitors and develop pharmacophore for enhanced activity.

Methods: The three-dimensional quantitative structure–activity relationship (3D-QSAR), docking and pharmacophore identification studies on 2-amino-pyrazolopyridine derivatives as plk1 inhibitors have been carried out using V Life MDS 4.3 software. The stepwise 3D-QSAR *k*NN-MFA method was applied to derive QSAR model. Also, ADMET prediction was performed using FAF Drugs 2 which runs on Linux OS.

Results: The information rendered by 3D-QSAR models may lead to a better understanding and designing of novel plk1 inhibitor molecules. The molecular docking analysis was carried out to better understand the interactions between plk1 enzyme and inhibitors in this series. Hydrophobic and hydrogen bond interactions lead to identification of active binding sites. The results of pharmacophore studies showed that hydrogen bond accepters, aromatic and aliphatic centers are the important features for polo-like kinase 1 inhibitor activity. ADMET prediction of these compounds showed good drug like properties.

Conclusion: The combination of the 3D-QSAR, docking, pharmacophore modeling and ADMET prediction is an important tool in understanding the structural requirements for design of novel, potent and selective plk1 inhibitors and can be employed to design new drug discovery and can be used for derivatives of 2-amino-pyrazolopyridines with specific plk1 inhibitory activity.

Keywords: Polo-like kinase 1 inhibitors, 3D-QSAR, *k*NN-MFA model, Docking study, Pharmacophore modeling, ADMET properties.

INTRODUCTION

Molecular modeling study is an approach that has been used to narrow down a library containing an extraordinarily high number of random molecules into a smaller list of the potentially effective inhibitors [1]. Quantitative-structure activity relationship (QSAR) studies leading to models in terms of chemical structures and their biological activities are a powerful tool for drug design in medicinal chemistry [2]. Three dimensional quantitative structure–activity relationships (3D-QSAR) is a widely used model for identification of the steric, electrostatic and hydrophobic structural requirements of various drugs acting via receptor modulation for exerting their biological activity. By the application of 3D-QSAR models, the number of compounds that need to be synthesized by a medicinal chemist can be reduced greatly. Thus, the time and cost of drug discovery and development can also be reduced [3]. The molecular docking study is used as an important tool in drug discovery to better understand the interactions between the ligands and receptors. Pharmacophore modeling is also an important model and widely used in drug discovery process to correlate the observed biological activities for a series of compounds with their chemical structures. Such a model could also be used as a query for screening chemical databases to find new chemical entities. Now a days, *in silico* ADMET prediction have become an essential requirement for screening the drugs before further screening for biological activities.

Polo-like kinases (plks) are an evolutionarily conserved family of serine/threonine kinases characterized by an amino-terminal serine/threonine kinase domain and carboxy-terminal polo box domain(s). The plks family includes plk1, plk2 (SNK), plk3 (PRK/FNK), plk4 (SAK) and More recently, plk5 has been identified; however, it lacks a kinase domain and does not seem to function in cell cycle regulation. The plk1 plays an important role throughout mitosis and is involved in the regulation of mitotic progression, including mitotic entry, spindle formation, chromosome segregation and cytokinesis [4, 5]. The plk1 is the most investigated member of

the family and has been widely considered as an anticancer target [6–8]. The pharmacologic inhibition of plk1 in tumor cells results in defects in centrosome maturation and separation, mitotic spindle formation and chromosome alignment, leading to disruption of cell mitosis and even apoptosis [9–11]. The plk1 is over expressed in a broad range of human tumors and this over expression is positively correlated with aggressiveness and poor prognosis in many cancers. Thus, plk1 is considered as a good target for chemotherapeutic intervention [12-14]. With the above facts and in continuation of our research for identification of bioactive agents [15-16] in the present study, we reported 3D-QSAR, molecular docking, pharmacophore modeling and ADMET prediction of 2-aminopyrazolopyridine derivatives as plk1 inhibitors to provide further insight into the key structural features required to design potential drug candidates of this class. The output of present research work is interesting and can be further studied to develop potential plk1 inhibitors.

MATERIALS AND METHODS

Data sets and biological activity

All molecular modeling studies (3D-QSAR, molecular docking, and pharmacophore model) were performed using the molecular modeling software package VLife Molecular Design Suite (VLife MDS) version 4.3 [17] on HP-PC (HPLV1911) with a Pentium IV processor and Windows 7 operating system. A dataset of 2-aminopyrazolopyridine derivatives with reported activities was used in present study [18]. Since some compound exhibited insignificant/no inhibition, such compounds were excluded from the present study. The structures and their inhibitory activities in IC₅₀ (μM) are listed in table 1.

Ligand preparation

2D structure of 2-aminopyrazolopyridine derivatives was drawn using VLife2 Draw tool. All structures were cleaned and 3D optimized. All the 3D structures were optimized using Merck

molecular force field (MMFF) [19] with distance dependent dielectric function and energy gradient of 0.01 kcal/mol Å with 10000 numbers of cycles. The total energy of a conformation can be calculated using MMFF by the relation;

$$E_{\text{total}} = E_B + E_A + E_{BA} + E_{\text{OOP}} + E_T + E_{\text{vdw}} + E_{\text{elec}}$$

Where,

E_B = energy of bond stretching;

E_A = energy of angle bending;

E_{BA} = energy of bond stretching and angle bending;

E_{OOP} = out-of-plane bending energy;

E_T = torsion energy term;

E_{vdw} = van der Waals energy;

E_{elec} = electrostatic energy.

The conformers for all structures were generated and the low energy conformer for each compound was selected and used for further study.

3D-QSAR studies

Alignment of molecules

The molecules of the dataset were aligned by the template based technique, using the common structure of 2-aminopyrazolopyridine

derivatives with the help of VLife MDS 4.3 template based alignment tool. This method is based on moving the molecules in 3D space, which is related to the conformational flexibility of molecules. The goal is to obtain optimal alignment between the molecular structures necessary for ligand-receptor interactions [20].

The most active molecule was selected as a template for alignment of the molecules. A highly bioactive energetically stable conformation in this class of compounds is chosen as a reference molecule on which other molecules in the data set are aligned, considering template as a basis for the alignment.

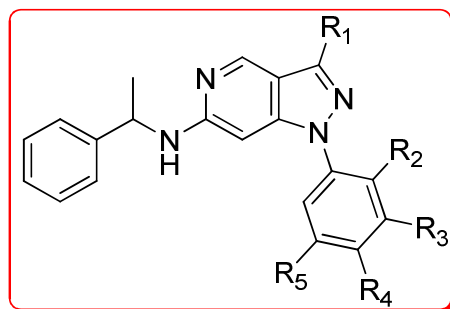


Table 1: Structures and biological activity of 2-amino-pyrazolopyridine derivatives

Code	R ₁	R ₂	R ₃	R ₄	R ₅	IC ₅₀ (μM)
1	H	H	H	H	H	1.301
2	H	CH ₃	H	H	H	7.685
3	H	H	CH ₃	H	H	0.474
4	H	H	H	CH ₃	H	4.528
5	OCH ₃	H	H	H	H	14.451
6	H	H	H	H	OCH ₃	5.928
7	H	H	H	OCH ₃	H	0.703
8	H	F	H	H	H	4.516
9	H	H	F	H	H	0.464
10	H	H	H	F	H	3.241
11	H	H	Cl	H	H	0.121
12	H	H	CH ₃ CHCH ₃	H	H	1.476
13	H	H	CN	H	H	0.412
14	H	H	N(CH ₃) ₂	H	H	0.977
15	H	H	SO ₂ CH ₃	H	H	0.225
16	H	H	CH ₃	H	CH ₃	0.149
17	H	H	Cl	H	Cl	0.641
18	H	H	Cl	H	Br	0.274
19	CH ₃	H	CH ₂ CH ₂ COOH	H	H	0.021
20	CH ₃	H	CH ₂ CH ₂ CONH ₂	H	H	0.032
21	CH ₃	H	CH ₂ CH ₂ CH ₂ NH ₂	H	H	0.059
22	CH ₃	H	2-PhCH ₂ CONH ₂	H	H	0.207
23	CH ₃	H	2-PhCONH ₂	H	H	0.042

3D-QSAR kNN-MFA model

Like many 3D-QSAR methods, k-nearest neighbor molecular field analysis (kNN-MFA) requires suitable alignment of given set of molecules [21]. This is followed by generation of a common rectangular grid around the molecules.

The steric and electrostatic interaction energies are computed at the lattice points of the grid using a methyl probe of charge +1. These interaction energy values are considered for the relationship generation and utilized as descriptors to decide nearness between molecules. The term descriptor is utilized in the following discussion to indicate field values at the lattice points. The optimal training and test sets were generated using the sphere exclusion algorithm. This algorithm allows the construction of training sets covering descriptor space occupied by representative points. Once the training and test sets were generated, kNN methodology was applied to the descriptors generated over the grid. The standard kNN method is implemented simply as follows:

- Calculate distances between an unknown object and all the objects in the training set,
- Select k objects from the training set most similar to object u, according to the calculated distances, and
- Classify object u with the group to which the majority of the k objects belong.

An optimal k value is selected by optimization through the classification of a test set of samples or by leave-one out cross-validation. kNN-MFA with stepwise (SW) variable selection method was used to generate 3D-QSAR equations. This method employs a stepwise variable selection procedure combined with kNN to optimize (i) the number of nearest neighbors (k) and (ii) the selection of variables from the original pool. The step by-step search procedure begins by developing a trial model with a single independent variable and adds independent variables, one step at a time, examining the fit of the model at each step. The method continues until there are no more significant variables remaining outside the model.

Molecular docking study

The VLifeMDS 4.3 BioPredicta tool was used to evaluate the binding free energy of the inhibitors against the plk1 receptor to gain insight into the binding modes of 2-aminopyrazolopyridines.

Selection and preparation of ligands and target protein crystal structures

The ligands (2-aminopyrazolopyridine) were studied for their binding activities into plk1 enzyme. The 2D structures of plk1 inhibitors were drawn using VLife2Draw 1.0 and converted to 3D conformations. The conformers thus obtained, were optimized (MMFF) till they reached a rms gradient energy of 0.001 kcal/mol. Å. The crystal structure of plk1 in complex with wortmannin (3D5X; resolution: 2.80 Å) was extracted from the RCSB Protein Data Bank [22]. All bound water molecules and ligands were removed from the proteins and polar hydrogens were added. The protein structure was energy minimized using Merck molecular force field (MMFF) with distance dependent dielectric function and energy gradient of 0.01 kcal/mol Å with 10000 numbers of cycles [19].

Identification of cavities

The cavities in the receptor were mapped to assign an appropriate active site. The basic features used to map the cavities were the surface mapping of the receptor and identifying the geometric voids as well as scaling the void for its hydrophobic characteristics using V Life MDS analyze tool. Hence all the cavities that are present in plk1 receptor are identified and ranked based on their size and hydrophobic surface area. Considering the dimensions and hydrophobic surface area, cavity-1 was found to be the best void as an active site residues (ILE26, ARG43, PHE44A, LEU45, GLY46, LYS47, GLY48, GLY49, PHE50A, ALA51, LYS52, CYS53, TYR54, GLU55, ILE56, PHE65, ALA66, GLY67, LYS68, VAL69, VAL70, PRO71, LYS72, MET74, LEU75, GLN80, LYS83, MET84, GLU87, ILE88, ILE90, HIS91, LEU94, VAL100, GLY101, PHE102, HIS103, GLY104, PHE105, ASP108, ASP110, PHE111, VAL112, TYR113, VAL114, VAL115, LEU116, GLU117, ILE118, CYS119, ARG120, ARG121, ARG122, SER123, LEU124, LEU125, GLU126, LEU153, VAL158, HIS160A, LYS164, LEU165, GLY166, ASN167, LEU168, PHE169, LEU170, LYS177, ILE178, GLY179, ASP180, PHE181, GLY182, and ALA184).

Run of docking study

The genetic algorithm (GA) docking of the conformers of each plk1 inhibitors into the plk1 protein was done by positioning with the active site of cavity-1 using V Life MDS 4.3 package following the standard operating procedures [17]. The complexes were energy minimized using the MMFF method, till they reached an rms gradient of 0.1 kcal/mol. Å. The binding energy in kcal/mol or the ligand-receptor interaction energy obtained after docking the ligands into the enzyme active site can be defined as:

$$E = \text{InterEq} + \text{InterEvdW} + \text{IntraEq} + \text{IntravdW} + \text{IntraEtor}$$

Where,

InterEq= Intermolecular electrostatic energy of complex;

InterEvdW= Intermolecular vdW energy of complex;

IntraEq= Intramolecular electrostatic energy of ligand;

IntraEvdW= Intramolecular vdW energy of ligand and

IntraEtor= Intramolecular torsion energy of ligand.

Pharmacophore modeling

Pharmacophore is defined as the minimum functionality that a molecule has to contain in order to exhibit activity. Pharmacophore mapping was carried out by means of the MolSign Module of VLife MDS 4.3. All aligned molecules were taken for pharmacophore development. The most active molecule **19** was selected to set it as the reference. The reference molecule is the molecule on which the other molecules of the align dataset get aligned. All spheres in the snapshot indicate all possible pharmacophoric centers and their color codes are as follows: blue color, hydrogen bond acceptor;

golden color, aromatic feature; and brown color, aliphatic group. This pharmacophore model can serve as an effective search filter for virtual screening.

ADMET prediction

ADMET prediction for the various physicochemical descriptors and pharmaceutically relevant properties was performed using FAFDrugs2 which runs on Linux OS [23]. This tool is freely available and used for *in silico* ADMET filtering. This approach has been widely used as a filter for substances that would likely be further developed in drug design programs. In particular, we calculated the compliance of compounds to the Lipinski's rule of five [24] and Veber's rule [25]. We have also assessed the parameters like number of rotatable bonds (>10) and number of rigid bonds which signify that compound may have good oral bioavailability and good intestinal absorption [26].

RESULTS AND DISCUSSION

3D-QSAR studies

In the present study, kNN-MFA model is developed coupled with stepwise variable selection method to develop 3D-QSAR models of 2-amino-pyrazolopyridines as plk1 inhibitors based on steric and electrostatic fields. The structure of 2-amino-pyrazolopyridine template is shown in figure 1. A highly bioactive energetically stable conformation in this class of compounds is chosen as a reference molecule on which other molecules in the data set are aligned, considering template as a basis for the alignment. The aligned view of 2-amino-pyrazolopyridines is presented in figure 2. The total data set was divided into training and test sets using the sphere exclusion algorithm for diversity of the sampling procedure. This approach resulted in selection of compounds **2, 3, 4, 10, 11, 14, and 17** as the test set and the remaining 16 compounds as the training set (table 2). Selection of molecules in the training set and test is a key and important feature of any QSAR model. Therefore the care was taken in such a way that biological activities of all compounds in test lie within the maximum and minimum value range of biological activities of training set of compounds. The UniColumn statistics for training set and test set were generated to check correctness of selection criteria for trainings and test set molecules and result reflected the correct selection of test and training sets (table 3). Several statistically significant 3D-QSAR models using stepwise variable selection method were generated, of which the corresponding best model is reported herein. The best 3D-QSAR kNN MFA model selected based on the value of statistical parameters has a $q^2 = 0.7187$ and $\text{pred}_r^2 = 0.2075$ (table 4).

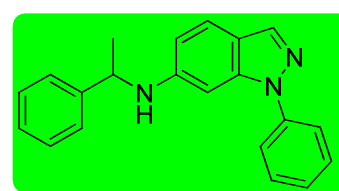


Fig. 1: 2-Amino-pyrazolopyridine (template)

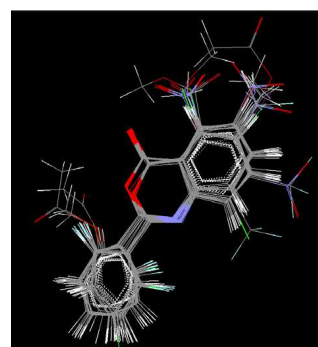


Fig. 2: Alignment of the molecules

Table 2: Observed and predicted activity by QSAR equation along with residuals and docking statistics

Code	Sets	pIC ₅₀		Residual	Docking statistics	H-bonds
		Exp.	Pred.			
1	Training	-0.114	0.015	-0.129	-3.369	GLY49-NH; GLY49-N=C
2	Test	-0.885	-0.395	-0.49	-3.371	GLY49-NH; GLY49-N=C
3	Test	0.324	-0.356	0.68	-7.937	GLY49-N=C
4	Test	-0.655	0.464	-1.119	-26.677	GLY49-NH; GLY49-N=C
5	Training	-1.159	-0.142	-1.017	4.432	PHE50-NH
6	Training	-0.772	-0.528	-0.244	-14.962	GLY49-NH; GLY49-N=C; LYS47-O-CH ₃
7	Training	0.153	0.533	-0.38	-16.480	GLY49-N=C
8	Training	-0.654	-0.256	-0.398	-2.857	GLY49-N=C
9	Training	0.333	0.358	-0.025	-26.413	GLY49-NH; GLY49-N=C
10	Test	-0.510	0.395	-0.905	-22.299	GLY49-NH; GLY49-N=C
11	Test	0.917	0.397	0.52	-23.755	GLY49-N=C
12	Training	-0.169	-0.014	-0.155	-22.860	*
13	Training	0.385	0.034	0.351	-3.714	GLY49-NH; PHE50-NH
14	Test	0.010	-0.395	0.405	-21.763	LYS47-N(CH ₃) ₂ ; GLY49-N=C
15	Training	0.647	0.739	-0.092	-23.524	LYS47-SO ₂ CH ₃ ; LYS47-O=S; GLY49-N=C
16	Training	0.826	0.353	0.473	-15.242	*
17	Test	0.193	0.398	-0.205	-17.670	GLY49-NH; GLY49-N=C
18	Training	0.562	0.299	0.263	-17.482	GLY49-N=C
19	Training	1.677	1.359	0.318	-44.363	GLY49-N=C; LYS47-OH
20	Training	1.494	1.434	0.060	-50.900	PHE50-NH; SER123-NH ₂ ; GLU126-NH ₂
21	Training	1.229	1.580	-0.351	-37.191	GLY49-NH; PHE50-NH; SER123-NH ₂ ; GLU126-NH ₂
22	Training	0.684	0.754	-0.070	-34.859	GLY49-NH
23	Training	1.376	0.467	0.909	-27.655	PHE50-NH

Exp.: Experimental activity; Pred.: Predicted; (*) denotes no hydrogen bond interaction of ligands with protein.

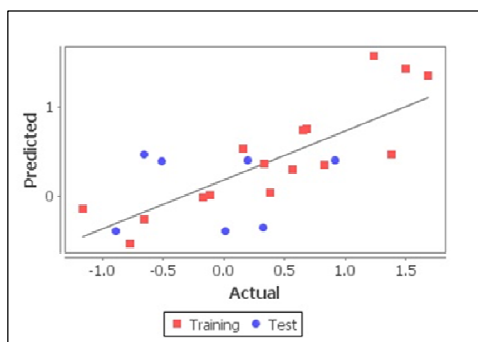
Table 3: Uni Column statistics of the training and test sets for QSAR models

Data set	Column name	Average	Max.	Min.	Std. deviation	Sum
Training	pIC ₅₀	0.4063	1.6780	-1.1600	0.8327	6.5000
Test	pIC ₅₀	-0.0870	0.9170	-0.8860	0.6333	-0.6090

Table 4: Statistical results of 3D-QSAR kNN MFA model generated by stepwise variable selection method

S. No.	Statistical parameter	Results
1	n (Training/Test)	16/7
2	k Nearest Neighbor	4
3	N	16
4	Degree of freedom	13
5	q ²	0.7187
6	q ² _{se}	0.4416
7	Predr ²	0.2075
8	pred_r ² _{se}	0.7368
9	Descriptors(Range)	S_1021-0.0542-0.0488 S_853 0.0400 0.2043

From table 2, it is evident that predicted activities of all the compounds are in good agreement with their corresponding experimental activities. The plots of observed versus predicted activity of both training & test sets molecules helped in cross-validation of kNN-MFA QSAR model and are depicted in figure 3.

**Fig. 3: Comparison of observed activity versus predicted activity for training set & test set compounds according to 3D-QSAR model by SW-kNN MFA method**

From stepwise 3D-QSAR kNN-MFA (SW-kNN MFA) model (table 4, figure 4), the points generated are S_1021 (-0.0542 -0.0488) and S_853 (0.0400 0.2043) i.e. steric interaction at their corresponding spatial grid points. These points suggested the significance and requirement of steric properties for better biological activities. It is observed that negative range at grid point S_1021 on phenyl moiety indicating that negative steric potential is favorable for increase in the activity of 2-amino-pyrazolopyridine derivatives and hence less bulky substituents are preferred in that region.

Therefore, less steric groups like -H and -CH₃ will be preferable for enhancing biological activity. Positive range at S_853 grid point on phenyl moiety indicates that positive steric potential is favorable for increase in the activity and hence more bulky substituent groups are preferred in that region.

Therefore bulky substituents such as -C₆H₅CONH₂, -CH₂CH₂COOH, -CH₂CH₂CH₂NH₂, and -CH₂CH₂CONH₂ etc. were preferred at the position of generated data point S_853 around 2-amino-pyrazolopyridines pharmacophore for maximum activity. These results are in close agreement with the experimental observations that compounds 12, 14, 15, 19, 20, 21, 22 and 23 with bulky substituent at R₃ position and less steric groups at R₄ of phenyl ring showed greater plk1 inhibitory activities (figure 5).

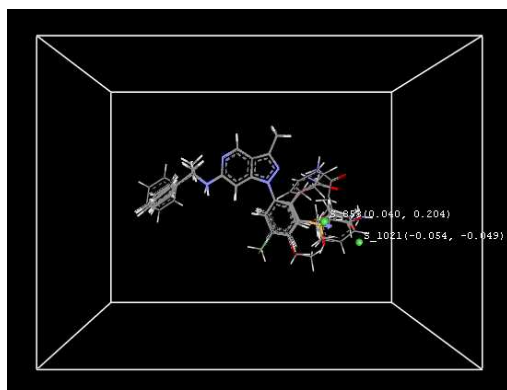


Fig. 4: Stereo view of the molecular rectangular field grid around the superposed molecular units of 2-amino-pyrazolopyridines series of compounds using SW-kNN MFA method

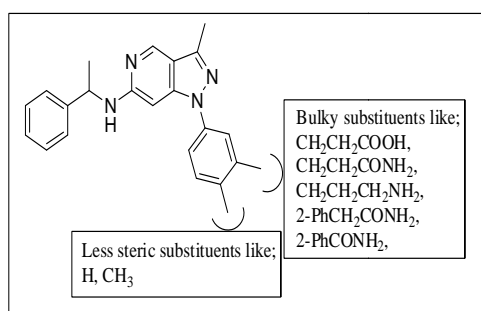


Fig. 5: Various substituents for better plk1 inhibitory activity

Thus, the contribution plot arising out of 3D-QSAR studies provide some useful insights for better understanding of the structural features of these compounds responsible for producing significant plk1 inhibitory activity, which conforms to the docking results.

Molecular docking study

The molecular docking was performed to establish the molecular basis of 2-amino-pyrazolopyridine derivatives as Polo-like kinase 1 inhibitors. All the 23 reported compounds 2-amino-pyrazolopyridines series were docked against plk1 receptor. The docking calculation and hydrogen bond interactions are shown in table 2. The docking results indicated that these compounds held in the active pocket by combination of hydrophobic and van der Waals interactions with the protein. Major hydrophobic contacts occurred between the plk1 inhibitors with the side chain of GLY46, LYS47, GLY48, GLY49, PHE50, SER123, LEU125, LYS164 and GLY166. The hydrogen bond interaction was observed with amino acids residues like LYS47, GLY49, PHE50, SER123 and GLU126. The compounds **12**, **14**, **15**, **19**, **20**, **21**, **22** and **23** with bulky substituents at R₃ position and less steric groups at R₄ position of phenyl ring have shown good binding interactions energy and bulky substituents are held in active site by forming hydrophobic bonds. Thus, docking study is also confirming our 3D-QSAR model study. The most active compounds **19** and **20** (IC₅₀= 0.032, and 0.021 μM, respectively) have shown lowest binding energy i.e. -44.363 and -50.90 kcal/mol, respectively (figure 6).

Pharmacophore modeling

A set of pharmacophore hypothesis was generated using the MolSign module of VLife MDS 4.3. We generated different pharmacophore patterns based on a set of 23 aligned molecules. It starts generating properties of molecules and finds the common three dimensional map of three to maximum common properties. All the possible pharmacophore models are aligned automatically and alignment is done on the basis of common properties.

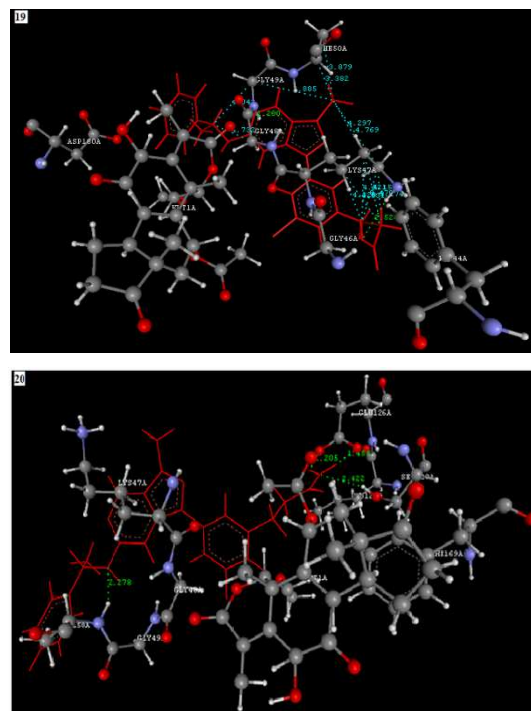


Fig. 6: Docking study of compounds 19 and 20 with plk1 (PDB ID: 3D5X). Ligands are shown in red color. Hydrogen bonds are shown in green color. Hydrophobic bonds are shown in sky blue color

Each hypothesis was found to contain common features like aliphatic (brown color), aromatic (golden color) and hydrogen bond acceptor (blue color). The results of pharmacophore identification studies are given in figure 7. Structure and pharmacophoric features of 2-amino-pyrazolopyridine derivatives indicated that the designed set of molecules is having hydrogen bond acceptor (blue color), aromatic features (golden color) and aliphatic feature (brown color) in common. The distances among the various chemical features are as follows:

- Aliphatic carbon centre-Hydrogen bond acceptor = 4.655 Å
- Aliphatic carbon centre- Aromatic carbon centre 1 = 3.284 Å
- Aliphatic carbon centre- Aromatic carbon centre 2 = 6.284 Å
- Aromatic carbon centre 1- Hydrogen bond acceptor = 1.896 Å
- Aromatic carbon centre 1- Aromatic carbon centre 2 = 4.875 Å
- Hydrogen bond acceptor- Aromatic carbon centre 2 = 6.699 Å

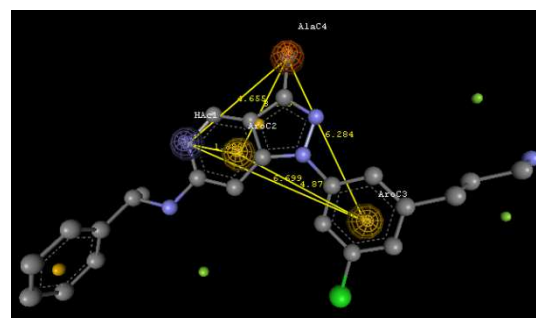


Fig. 7: Common pharmacophore and distance between pharmacophoric features for 2-amino-pyrazolopyridine derivatives as plk1 inhibitors

ADMET prediction

All the compounds showed significant values for the various parameters analyzed and showed good drug-like characteristics based on Lipinski's rule of five (table 5). The 23 compounds were

within the range of accepted values. None of the compounds had violated Veber rule (Rotatable bonds ≤ 10 and PSA ≤ 140). The compounds except **1**, **5**, **6**, **7**, **13**, **19**, **22**, and **23** had violated one rule i.e. $\log p \geq 5$ of the Lipinski's rule. A molecule likely to be developed as an orally active drug candidate should show no more than one violation of the following four criteria: $\log P$ (octanol-water

partition coefficient) ≤ 5 , molecular weight ≤ 500 , number of hydrogen bond acceptors ≤ 10 and number of hydrogen bond donors ≤ 5 . Thus, all these compounds followed the criteria for orally active drug and therefore, these compounds can be further developed as oral drug candidates. All the compounds except **17**, **18**, and **21** were non toxic.

Table 5: Prediction of ADMET properties of compounds

Code	MW	$\log p$	PSA	Rot. bond	Rig.bond	HBD	HBA	Lipinski violation	Veber violation	Toxicity
1	328.41	4.97	42.74	4	22	1	2	0	FALSE	NT
2	342.43	5.28	42.74	4	22	1	2	1	FALSE	NT
3	342.43	5.28	42.74	4	22	1	2	1	FALSE	NT
4	342.43	5.28	42.74	4	22	1	2	1	FALSE	NT
5	358.43	4.98	51.97	5	22	1	3	0	FALSE	NT
6	358.43	4.98	51.97	5	22	1	3	0	FALSE	NT
7	358.43	4.98	51.97	5	22	1	3	0	FALSE	NT
8	346.40	5.11	42.74	4	22	1	2	1	FALSE	NT
9	346.40	5.11	42.74	4	22	1	2	1	FALSE	NT
10	346.40	5.11	42.74	4	22	1	2	1	FALSE	NT
11	362.85	5.62	42.74	4	22	1	2	1	FALSE	NT
12	370.49	6.09	42.74	5	22	1	2	1	FALSE	NT
13	353.41	4.84	66.53	4	23	1	2	0	FALSE	NT
14	371.47	5.04	45.98	5	22	1	2	1	FALSE	NT
15	406.50	5.45	85.26	5	24	1	4	1	FALSE	NT
16	356.46	5.59	42.74	4	22	1	2	1	FALSE	NT
17	397.30	6.28	42.74	4	22	1	2	1	FALSE	T
18	441.75	6.39	42.74	4	22	1	2	1	FALSE	T
19	434.91	4.64	80.04	7	23	2	4	0	FALSE	NT
20	433.93	4.74	85.83	6	24	2	3	0	FALSE	NT
21	419.94	6.22	68.76	7	22	2	2	1	FALSE	T
22	496.00	4.92	85.83	6	30	2	3	0	FALSE	NT
23	481.97	4.89	85.83	5	30	2	3	0	FALSE	NT

MW: molecular weight; $\log p$: logarithm of partition coefficient of compound between n-octanol and water; PSA: polar surface area; Rot. bond: rotatable bond; Rig. bond: rigid bond; HBD: hydrogen bond donor; HBA: hydrogen bond acceptor; T: toxic; NT: non toxic.

CONCLUSION

The stepwise method is applied for optimization and selection of suitable descriptors for development of 3D-QSAR kNN-MFA model for a series of 2-amino-pyrazolopyridine derivatives as polo-like kinase 1 inhibitors using VLifeMDS 4.3 drug design software. The 3D-QSAR results revealed that bulky substituent at R₃ position and less steric groups at R₄ position of phenyl ring were preferred for enhancing biological activity of 2-amino-pyrazolopyridine analogs. This finding supports the experimental observations, where presence of bulky groups at R₃ and less steric groups at R₄ position of phenyl ring signifies increase in activities of compounds. From the molecular docking studies, it is evident that bulky groups at R₃ position of phenyl ring of 2-amino-pyrazolopyridines forms strong hydrophobic interactions with active site of hydrophobic amino acid residues. The pharmacophore patterns of 2-amino-pyrazolopyridine derivatives were developed using MolSign Module of VLife MDS 4.3. The chemical feature based best common pharmacophore has two aromatic carbon centers, one aliphatic carbon center, one hydrogen bond acceptor features. The ADMET prediction revealed that compounds can be further developed as good oral drug candidates. Hence, the combination of the above studies (3D-QSAR, docking, pharmacophore modeling, and ADMET prediction) are useful in understanding the structural requirements for design of novel, potent and selective plk1 inhibitors and can be employed to design new derivatives 2-amino-pyrazolopyridines with specific plk1 inhibitory activity.

ACKNOWLEDGMENTS

The authors are thankful to Mrs. Fatima Rafiq Zakaria, Chairman, Maulana Azad Educational Trust and Principal, Y.B. Chavan College of Pharmacy, Dr. Rafiq Zakaria Campus, Aurangabad 431 001 (M.S.), India for providing the facility.

CONFLICT OF INTERESTS

The authors confirm that this article content has no conflicts of interest.

REFERENCES

- Jain SV, Bhadoriya KS, Bari SB, Sahu NK, Ghate M. Discovery of Potent Anticonvulsant Ligands as Dual NMDA and AMPA Receptors Antagonists by Molecular Modeling Studies. *Med Chem Res* 2012;21 (11):3465-84.
- Hadjipavlou-Litina D. Review, Reevaluation, and New Results in Quantitative Structure-Activity Studies of Anticonvulsants. *Med Res Rev* 1998;18 (2):91-119.
- Bhadoriya KS, Jain SV, Bari SB, Chavhan ML, Vispute KR. 3D-QSAR Study of Indol-2-yl Ethanones Derivatives as Novel Indoleamine 2,3-Dioxygenase (IDO) Inhibitors. *J Chem* 2012;9 (4):1753-59.
- Barr FA, Sillje HHW, Nigg EA. Polo-Like Kinases and the Orchestration of Cell Division. *J Nat Rev Mol Cell Biol* 2004;5 (6):429-41. (b) Glover DM, Hagan IM, Tavares AAM. Polo-Like Kinases: A Team that Plays Throughout Mitosis. *Genes Dev* 1998;12 (24):3777-87.
- De Carcer G, Escobar B, Higuero AM, Garcia L, Anson A, Perez G, et al. Plk5, A Polo Box Domain-Only Protein with Specific Roles in Neuron Differentiation and Glioblastoma Suppression. *Mol Cell Biol* 2011;31 (6):1225-39.
- Degenhardt Y, Lampkin T. Targeting Polo-like Kinase in Cancer Therapy. *Clin Cancer Res* 2010;16 (2):384-89.
- Strebhardt K, Ullrich A. Targeting Polo-Like Kinase 1 for Cancer Therapy. *Nat Rev Cancer* 2006;6 (4):321-30.
- Strebhardt K. Multifaceted Polo-Like Kinases: Drug Targets and Antitargets for Cancer Therapy. *Nat Rev Drug Discov* 2010;9 (8):643-60.
- Steehmaier M, Hoffmann M, Baum A, Lenart P, Petronczki M, Krssak M, et al. BI 2536, a Potent and Selective Inhibitor of Polo-Like Kinase 1, Inhibits Tumor Growth *in Vivo*. *Curr Biol* 2007;17 (4):316-22.
- Elez R, Piiper A, Kronenberger B, Kock M, Brendel M, Hermann E, et al. Tumor Regression by Combination Antisense Therapy Against Plk1 And Bcl-2. *Oncogene* 2003;22 (1):69-80.

11. Spankuch-Schmitt B, Wolf G, Solbach C, Loibl S, Knecht R, Stegmüller M, *et al.* Downregulation of Human Polo-Like Kinase Activity by Antisense Oligonucleotides Induces Growth Inhibition in Cancer Cells. *Oncogene* 2002;21 (20):3162-71.
12. Eckerdt F, Yuan J, Strebhardt K. Polo-Like Kinases and Oncogenesis. *J Oncogene* 2005;24 (2):267-76.
13. Takai N, Hamanaka R, Yoshimatsu, Miyakawa I. Polo-Like Kinases (Plks) and Cancer. *Oncogene* 2005;24 (2):287-91.
14. Strebhardt K, Ullrich A. Targeting Polo-Like Kinase 1 for Cancer Therapy. *Nat Rev Cancer* 2006;6 (4):321-30.
15. Sangshetti JN, Shinde DB. Synthesis of Some Novel 3-(1-(1-Substitutedpiperidin-4-yl)-1*H*-1,2,3-triazol-4-yl)-5-substituted phenyl-1,2,4-oxadiazoles as Antifungal Agents. *Eur J Med Chem* 2011;46 (4):1040-44. (b) Sangshetti JN, Nagawade RR, Shinde DB. Synthesis of Novel 3-(1-(1-Substitutedpiperidin-4-yl)-1*H*-1,2,3-triazol-4-yl)-1,2,4-oxadiazol-5(4*H*)-one as Antifungal Agents. *Bioorg Med Chem Lett* 2009;19 (13):3564-67. (c) Sangshetti JN, Shinde DB. One Pot Synthesis and SAR of Some Novel 3-Substituted-5,6-diphenyl-1,2,4-triazines as Antifungal Agents. *Bioorg Med Chem Lett* 2010;20 (2):742-45. (d) Sangshetti JN, Dharmadhikari PP, Chouthe RS, Fatema B, Lad V, Karande V, Darandale SN, Shinde DB. Microwave Assisted Nano (ZnO-TiO₂) Catalyzed Synthesis of Some New 4,5,6,7-Tetrahydro-6-((5-substituted-1,3,4-oxadiazol-2-yl)methyl)thieno[2,3-*c*]pyridine as Antimicrobial Agents. *J Bioorg Med Chem Lett* 2013;23 (7):2250-53. (e) Sangshetti JN, Lokwani DK, Sarkate AP, Shinde DB. Synthesis, Antifungal Activity, and Docking Study of Some New 1,2,4-Triazole Analogs. *J Chem Biol Drug Des* 2011;78 (5):800-09.
16. Sangshetti JN, Chabukswar AR, Shinde DB. Microwave Assisted One Pot Synthesis of Some Novel 2,5-Disubstituted-1,3,4-oxadiazoles as Antifungal Agents. *Bioorg Med Chem Lett* 2011;21 (1):444-48. (b) Sangshetti JN, Shaikh RI, Khan FAK, Patil RH, Marathe SD, Gade WN, Shinde DB. Synthesis, Antileishmanial Activity and Docking Study of *N'*-Substitutedbenzylidene-2-(6,7-dihydrothieno[3,2-*C*]pyridin-5(4*H*)-yl)acetohydrazides. *Bioorg Med Chem Lett* 2014;24 (6):1605-10. (c) Sangshetti JN, Khan FAK, Chouthe RS, Damale MG, Shinde DB. Synthesis, Docking and ADMET Prediction of Novel 5-((5-Substituted-1-*H*-1,2,4-triazol-3-yl)methyl)-4,5,6,7-tetrahydrothieno[3,2-*C*]pyridine as Antifungal Agents. *Chinese Chem Lett* 2014;25 (7):1033-38.
17. VLife Molecular Design Suite 4.3, VLife Sciences Technologies Pvt. Ltd;www.Vlifesciences.com.
18. Fucini RV, Hanan EJ, Romanowski MJ, Elling RA, Lew W, Barr KJ, *et al.* Design and Synthesis of 2-Amino-pyrazolopyridines as Polo-Like Kinase 1 Inhibitors. *Bioorg Med Chem Lett* 2008;18 (20):5648-52.
19. Halgren TA. Molecular Geometries and Vibrational Frequencies for MMFF94. *J Comput Chem* 1996;17 (5-6):553-86.
20. Cramer RD, Patterson DE, Bunce JD. Comparative Molecular Field Analysis (CoMFA). 1. Effect of Shape on Binding of Steroids to Carrier Proteins. *Am Chem Soc* 1988;110 (18):5959-67.
21. Sharaf MA, Illman DL, Kowalski BR. *Chemometrics*. Wiley (NY);1986.
22. Elling RA, Fucini RV, Romanowski MJ. Structures of the Wild-Type and Activated Catalytic Domains of *Brachydanio Rerio* Polo-Like Kinase 1 (Plk1):Changes in the Active-Site Conformation and Interactions with Ligands. *Acta Crystallogr Sect D* 2008;64 (9):909-18.
23. Lagorce D, Sperandio H, Miteva MA, Villoutreix BO. FAF-Drugs2:Free ADME/Tox Filtering Tool to Assist Drug Discovery and Chemical Biology Projects. *BMC Bioinformatics* 2008;9:396.
24. Lipinski CA, Lombardo F, Dominy BW, Feeney PJ. Experimental and Computational Approaches to Estimate Solubility and Permeability in Drug Discovery and Development Settings. *Adv Drug Deliv Rev* 2001;46 (1-3):3-26.
25. Veber DF, Johnson SR, Cheng HY, Smith BR, Ward KW, Kopple KD. Molecular Properties That Influence the Oral Bioavailability of Drug Candidates. *J Med Chem* 2002;45 (12):2615-23.
26. Ertl P, Rohde B, Selzer P. Fast Calculation of Molecular Polar Surface Area as a Sum of Fragment-Based Contributions and Its Application to the Prediction of Drug Transport Properties. *J Med Chem* 2000;43 (20):3714-17.